SIAM J. SCI. COMPUT.
Vol. 28, No. 4, pp. 1289–1300

ENHANCING EIGENVALUE APPROXIMATION BY GRADIENT RECOVERY*

AHMED NAGA†, ZHIMIN ZHANG‡, AND AIHUI ZHOU§

Abstract. The polynomial preserving recovery (PPR) is used to enhance the finite element eigenvalue approximation. Remarkable fourth order convergence is observed for linear elements under structured meshes as well as unstructured initial meshes (produced by the Delaunay triangulation) with the conventional bisection refinement.

Key words. finite element method, recovery, superconvergence, eigenvalue

AMS subject classifications. 65N30, 65N15, 65N12, 65D10, 74S05, 41A10, 41A25

DOI. 10.1137/050640588

1. Introduction.

Recovery techniques such as the Zienkiewicz–Zhu superconvergence patch recovery (SPR) have been widely used in the finite element software industry for a posteriori error estimates and adaptive remeshing [1, 2, 14, 15]. Recently, we have discovered a new application for recovery techniques, which might have been overlooked in previous literature.

In this article, we report some remarkable enhancement results for the finite element eigenvalue approximation. The enhancement is based on gradient recovery techniques, especially the newly developed polynomial preserving recovery (PPR) [6, 7, 12, 13]. We know that the optimal convergence rate of the eigenvalue approximation by linear element for the Laplace operator is $O(h^2)$. Our numerical results indicate that the enhanced eigenvalue approximation converges at a rate of $O(h^4)$ for structured meshes as well as unstructured initial meshes (produced by the Delaunay triangulation) with regular refinement.

2. Eigenvalue enhancement.

On a domain $\Omega \subset \mathbb{R}^2$ with Lipschitz boundary, we consider a model eigenvalue problem: Find $(u, \lambda) \in H_0^1(\Omega) \times \mathbb{R}$ with $\|u\|_{0,\Omega} = 1$, such that

$$a(u, v) = \int_\Omega \nabla w \cdot \nabla v = \lambda(u, v) = \lambda \int_\Omega uv \quad \forall v \in H_0^1(\Omega). \tag{2.1}$$

We know that (2.1) has a countable sequence of real eigenvalues $0 < \lambda_1 \le \lambda_2 \le \cdots \to \infty$ and that their corresponding eigenfunctions are $u_1, u_2, \ldots$, which can be assumed to satisfy $(u_i, u_j) = \delta_{ij}$ for all $i, j \ge 1$.

The finite element approximation for (2.1) reads as follows: Find $(u_h, \lambda_h) \in S_0^h(\Omega) \times \mathbb{R}$ with $\|u_h\|_{0,\Omega} = 1$, such that

$$a(u_h, v_h) = \lambda_h(u_h, v_h) \quad \forall v_h \in S_0^h(\Omega) = S^h(\Omega) \cap H_0^1(\Omega), \tag{2.2}$$

*Received by the editors September 18, 2005; accepted for publication (in revised form) February 16, 2006; published electronically July 31, 2006.
http://www.siam.org/journals/sisc/28-4/64058.html

†Applied Automation Technologies, Inc., Troy, MI 48083 (anaga@capps-edges.com).

‡Corresponding author. Department of Mathematics, Wayne State University, Detroit, MI 48202 (zzhang@math.wayne.edu). This author's work was supported in part by National Science Foundation grant DMS-0311807.

§Institute of Computational Mathematics and Scientific/Engineering Computing Academy of Mathematics and System Science, Chinese Academy of Sciences, Beijing 100080, China (azhou@lsec.cc.ac.cn).

where $S^h(\Omega)$ is the usual piecewise linear C^0 finite element space. It is well known that (2.2) has a finite sequence of eigenvalues $0 < \lambda_{1,h} \leq \lambda_{2,h} \leq \cdots \leq \lambda_{n_h,h}$ and corresponding eigenfunctions $u_{1,h}, u_{2,h}, \ldots, u_{n_h,h}$, where $(u_{i,h}, u_{j,h}) = \delta_{ij}$ for all $(1 \leq i, j \leq n_h)$ and $n_h = \dim S_0^h(\Omega)$. In addition (see, e.g., [3, 4]),

$$\lambda_{i,h} \geq \lambda_i, \quad i = 1, 2, \ldots, n_h. \tag{2.3}$$

The following identity of eigenvalue and eigenfunction approximation (see, e.g., [3, 10]) is crucial for our method.

LEMMA 2.1. *Let (u, λ) be the solution of (2.1). Then for any $w \in H_0^1(\Omega) \setminus \{0\}$, there holds*

$$\frac{a(w,w)}{\|w\|_{0,\Omega}^2} - \lambda = \frac{a(w-u, w-u)}{\|w\|_{0,\Omega}^2} - \lambda \frac{\|w-u\|_{0,\Omega}^2}{\|w\|_{0,\Omega}^2}. \tag{2.4}$$

Setting $w = u_h$ in (2.4) yields

$$\lambda_h - \lambda = \|\nabla(u - u_h)\|_{0,\Omega}^2 - \lambda \|u - u_h\|_{0,\Omega}^2. \tag{2.5}$$

2.1. The polynomial preserving recovery (PPR). Following Zhang and Naga [13], we introduce a PPR operator $G_h : S^h \longrightarrow S^h \times S^h$, which produces a continuous piecewise linear gradient field and satisfies the following two properties:

(1) Polynomial preserving: There exists a constant C independent of u and h, such that

$$\|\nabla u - G_h u_I\|_{0,\Omega} \leq Ch^2 |u|_{3,\Omega},$$

where $u_I \in S^h$ is the piecewise linear interpolation of u.

(2) Boundedness: There exists a constant C independent of v and h, such that

$$\|G_h v\|_{0,\Omega} \leq C|v|_{1,\Omega} \quad \forall v \in S^h.$$

We expect that the recovered gradient $\mathrm{G_h}\, u_h$ is "closer" to ∇u than ∇u_h is. Toward this end, we need some restriction on the mesh.

We say that two adjacent triangles (sharing a common edge) form an $O(h^{1+\alpha})$ $(\alpha > 0)$ approximate parallelogram if the lengths of any two opposite edges differ by only $O(h^{1+\alpha})$.

DEFINITION. *The triangulation $\mathcal{T}_h$ is said to satisfy* Condition α *if any two adjacent triangles form an $O(h^{1+\alpha})$ parallelogram.*

A common mesh refinement strategy is the *bisection*, which decomposes one triangle into four congruent subtriangles by linking the three edge centers. An important property of the bisection is that it satisfies *Condition* α with $\alpha = \infty$.

We are able to establish the following theorem for the eigenfunction approximation. The proof will be omitted here since it is a straightforward mimic of proofs in [6, 9].

THEOREM 2.1. *Let $u \in W_\infty^3(\Omega) \cap H_0^1(\Omega)$ and $u_h \in S_0^h(\Omega)$ be the eigenfunctions of* (2.1) *and* (2.2)*, respectively. Let G_h be a recovery operator satisfying polynomial preserving and boundedness properties. Assume that the triangulation $\mathcal{T}_h$ satisfies* Condition α. *Then there exists a constant C independent of u and h, such that*

$$\|\nabla u - G_h u_h\|_{0,\Omega} \leq Ch^{1+\beta} \|u\|_{3,\infty,\Omega}, \qquad \beta = \min(\alpha, 1). \tag{2.6}$$

Remark. Although the theory needs some mesh condition, the recovery procedure itself can be applied to arbitrary meshes including anisotropic cases.

In what follows we also require that both u and a sequence of meshes $\mathcal{T}_h$ satisfy the following nondegeneracy property: There exists a constant $C > 0$ independent of h such that

$$\|\nabla(u - u_h)\|_{0,\Omega} \geq Ch. \tag{2.7}$$

As argued by Dörfler and Nochetto [5, sect. 4], this is not a very restrictive condition in practice; it is guaranteed, for instance, if $|D^2u(x)| \geq C > 0$ for all x in a fixed region of Ω.

2.2. Asymptotically exact error estimates for $\boldsymbol{\lambda_h - \lambda}$. An immediate benefit from the improved gradient based on the PPR is its accurate prediction of the error. We have the following theorem.

THEOREM 2.2. *Let the recovered gradient* $\mathrm{G_h}\, u_h$ *satisfy* (2.6). *Under the nondegeneracy condition* (2.7), *we have*

$$\eta_h^2(1 - Ch^\beta) \leq \lambda_h - \lambda \leq \eta_h^2(1 + Ch^\beta), \quad \eta_h = \|\mathrm{G_h}\, u_h - \nabla u_h\|_{0,\Omega}, \tag{2.8}$$

where $C > 0$ *is a constant independent of* (u, λ) *and* h.

Proof. To simplify the notation, we denote $e_h = u - u_h$. By the triangular inequality, we have

$$\|\nabla e_h\|_{0,\Omega} - \|\nabla u - \mathrm{G_h}\, u_h\|_{0,\Omega} \leq \eta_h \leq \|\nabla e_h\|_{0,\Omega} + \|\nabla u - \mathrm{G_h}\, u_h\|_{0,\Omega}.$$

Applying (2.6) and (2.7), we derive

$$1 - Ch^\beta \leq \frac{\eta_h}{\|\nabla e_h\|_{0,\Omega}} \leq 1 + Ch^\beta \tag{2.9}$$

or, equivalently,

$$1 - Ch^\beta \leq \frac{\|\nabla e_h\|_{0,\Omega}}{\eta_h} \leq 1 + Ch^\beta. \tag{2.10}$$

Recalling the identity (2.4), we obtain

$$\eta_h^2(1 - Ch^\beta) - \lambda\|e_h\|_{0,\Omega}^2 \leq \lambda_h - \lambda \leq \eta_h^2(1 + Ch^\beta) - \lambda\|e_h\|_{0,\Omega}^2.$$

Note that $\|e_h\|_{0,\Omega}^2 = O(h^4)$; there holds

$$\eta_h^2(1 - Ch^\beta) \leq \lambda_h - \lambda \leq \eta_h^2(1 + Ch^\beta),$$

with a different C. ∎

Note that η_h is computable and serves here as an a posteriori error estimator, which is asymptotically exact. This type of error estimator based on recovery is known as the Zienkiewicz–Zhu estimator [14, 15]. We refer readers to [1, 2] for the general theory of a posteriori error estimates in finite element methods.

Estimate (2.8) holds for any a posteriori error estimator η_h which satisfies (2.9). Thus the result of Theorem 2.2 is not restricted to gradient recovery.

2.3. Eigenvalue enhancement. Now we propose an enhanced eigenvalue approximation based on the PPR-recovered gradient:

$$\lambda_h^* = \lambda_h - \eta_h^2. \tag{2.11}$$

Note that the cost of computing quantity $\eta_h = \|\mathrm{G_h}\, u_h - \nabla u_h\|_{0,\Omega}$ is very low. We refer to [8] for a general defect correction approach to improve the approximation accuracy of eigenvalues and [11] for other eigenvalue improvement techniques. The emphasis here is on the PPR under arbitrary initial meshes and superconvergence.

THEOREM 2.3. *Let the recovered gradient* $\mathrm{G_h}\, u_h$ *satisfy* (2.6). *Under the nondegeneracy condition* (2.7)*, the enhanced eigenvalue approximation satisfies*

$$|\lambda_h^* - \lambda| \le Ch^{2+\beta}. \tag{2.12}$$

Proof. From (2.8) and the definition of λ_h^*, we see that

$$-Ch^\beta \eta_h^2 \le \lambda_h^* - \lambda \le Ch^\beta \eta_h^2. \tag{2.13}$$

By the nondegeneracy condition (2.7) and the equivalence between η_h and $\|e_h\|_{0,\Omega}$ (2.9), we get $\eta_h = O(h)$. The conclusion follows by using $\eta_h = O(h)$ in (2.13). ∎

By (2.5), we see that the optimal rate for the linear finite element approximation of the eigenvalue is $O(h^2)$. Therefore, Theorem 2.3 is a superconvergence result.

Under uniform triangular mesh of the regular or chevron pattern, we can prove (2.6) with $\beta = 1$ for the linear finite element; see [13]. Then, by Theorem 2.3, we have

$$|\lambda_h^* - \lambda| \le Ch^3.$$

However, our numerical tests indicate

$$|\lambda_h^* - \lambda| \approx Ch^4$$

for all four patterns of uniform triangulation (see Figure 3.1) as well as uniform equilateral triangulation, and for unstructured initial meshes (generated by the Delaunay triangulation) with the bisection refinement. It seems that the error estimates in Theorems 2.2 and 2.3 are not optimal. Our conjecture is that instead of (2.9), we actually have

$$1 - Ch^{2\beta} \le \frac{\eta_h}{\|\nabla e_h\|_{0,\Omega}} \le 1 + Ch^{2\beta}. \tag{2.14}$$

As a consequence, we should have

$$\eta_h^2(1 - Ch^{2\beta}) \le \lambda_h - \lambda \le \eta_h^2(1 + Ch^{2\beta}) \tag{2.15}$$

in Theorem 2.2 and

$$|\lambda_h^* - \lambda| \le Ch^{2(1+\beta)} \tag{2.16}$$

in Theorem 2.3. With the bisection mesh refinement, we have $\alpha = \infty$, $\beta = 1$, and therefore, $|\lambda_h^* - \lambda| \le Ch^4$.

To better understand this ultraconvergence (superconvergence with degree 2) phenomenon, let us reexamine

$$\begin{aligned}\eta_h^2 &= \|\mathrm{G_h}\, u_h - \nabla u + \nabla e_h\|_{0,\Omega}^2\\ &= \|\nabla e_h\|_{0,\Omega}^2 + \|\mathrm{G_h}\, u_h - \nabla u\|_{0,\Omega}^2 + 2(\nabla e_h, \mathrm{G_h}\, u_h - \nabla u).\end{aligned}$$

Note that

$$\|\nabla e_h\|_{0,\Omega}^2 \le Ch^4, \qquad \|\mathrm{G_h}\, u_h - \nabla u\|_{0,\Omega}^2 \le Ch^{2(1+\beta)}.$$

Using the Hölder inequality, we obtain only

$$\frac{|(\nabla e_h, \mathrm{G_h}\, u_h - \nabla u)|}{\|\nabla e_h\|_{0,\Omega}^2} \le Ch^\beta,$$

which does not take into account the cancellation in the integral. The real bound should be

$$\frac{|(\nabla e_h, \mathrm{G_h}\, u_h - \nabla u)|}{\|\nabla e_h\|_{0,\Omega}^2} \le Ch^{2\beta}. \tag{2.17}$$

Unfortunately, we are not able to prove (2.17) even for uniform meshes. Nevertheless, we are able to verify it indirectly via numerical experience. Toward this end, we define a quantity

$$\omega_{1,h} = |(\mathrm{G_h}\, u_h - \nabla u, \mathrm{G_h}\, u_h - \nabla u_h)|\,. \tag{2.18}$$

Note that

$$\begin{aligned}(\nabla e_h, \mathrm{G_h}\, u_h - \nabla u) &= (\mathrm{G_h}\, u_h - \nabla u, \nabla u - \mathrm{G_h}\, u_h) + (\mathrm{G_h}\, u_h - \nabla u, \mathrm{G_h}\, u_h - \nabla u_h)\\ &= (\mathrm{G_h}\, u_h - \nabla u, \mathrm{G_h}\, u_h - \nabla u_h) + O(h^{2(1+\beta)}).\end{aligned}$$

We see that $\omega_{1,h}$ provides an indirect way to verify (2.17).

Another way to understand the role of $\omega_{1,h}$ in the ultraconvergence phenomenon of $\lambda_h^* - \lambda$ is via the identity

$$\begin{aligned}\lambda_h^* - \lambda &= \|\nabla u - \mathrm{G_h}\, u_h\|_{0,\Omega}^2 + 2(\nabla u - \mathrm{G_h}\, u_h, \mathrm{G_h}\, u_h - \nabla u_h) - \lambda\|e_h\|_{0,\Omega}^2\\ &= \|\nabla u - \mathrm{G_h}\, u_h\|_{0,\Omega}^2 \pm 2\omega_{1,h} - \lambda\|e_h\|_{0,\Omega}^2. \end{aligned}\tag{2.19}$$

If the recovered gradient enjoys superconvergence, then the term with the lowest convergence rate in (2.19) is the mixed dot product whose absolute value is $2\omega_{1,h}$. Indeed, this term controls the convergence rate of $\lambda_h^* - \lambda$, and sometimes, it cancels the first term $\|\nabla u - \mathrm{G_h}\, u_h\|_{0,\Omega}^2$ in a favorable way. We will see this in our numerical test examples.

In addition, we shall numerically examine another quantity,

$$\omega_{2,h} = \left|\|\nabla e_h\|_{0,\Omega} + \eta_h + \frac{\lambda\|e_h\|_{L_2(\Omega)}^2}{2\eta_h}\right| \left|\|\nabla e_h\|_{0,\Omega} - \eta_h - \frac{\lambda\|e_h\|_{L_2(\Omega)}^2}{2\eta_h}\right|. \tag{2.20}$$

Note that both $\|\nabla e_h\|_{0,\Omega}$ and η_h are of order $O(h)$. From our numerical test examples in the next section, we will see that η_h cancels the major part of $\|\nabla e_h\|_{0,\Omega}$. The role of $\omega_{2,h}$ can be seen from the following identity:

$$\begin{aligned}\lambda_h^* - \lambda &= \|\nabla e_h\|_{0,\Omega}^2 - \eta_h^2\left(1 + \frac{\lambda\|e_h\|_{0,\Omega}^2}{\eta_h^2}\right)\\ &= \left(\|\nabla e_h\|_{0,\Omega} + \eta_h\sqrt{1 + \frac{\lambda\|e_h\|_{0,\Omega}^2}{\eta_h^2}}\right)\left(\|\nabla e_h\|_{0,\Omega} - \eta_h\sqrt{1 + \frac{\lambda\|e_h\|_{0,\Omega}^2}{\eta_h^2}}\right). \end{aligned}\tag{2.21}$$

Using the first two terms of the asymptotic expansion

$$\sqrt{1+\frac{\lambda\|e_h\|_{0,\Omega}^2}{\eta_h^2}} = 1 + \frac{\lambda\|e_h\|_{0,\Omega}^2}{2\eta_h^2} - \frac{\lambda^2\|e_h\|_{0,\Omega}^4}{4\eta_h^4} + \frac{3\lambda^3\|e_h\|_{0,\Omega}^6}{8\eta_h^6} + \cdots,$$

we have

$$\lambda_h^* - \lambda = \omega_{2,h} + \text{h.o.t.}$$

3. Numerical examples. In this section we numerically test the proposed eigenvalue enhancement procedure. The examples are based on the two-dimensional eigenvalue problem of (2.1). For comparison purposes, we compute the recovered gradient by both the PPR and Zienkiewicz–Zhu SPR [14].

Let λ denote the minimum eigenvalue and u the corresponding eigenfunction. As we mentioned before, if $\|\mathrm{G_h}\, u_h - \nabla u\|_{0,\Omega}$ has any superconvergence, then $\lambda_h^* - \lambda$ also has superconvergence. Indeed, this superconvergence is attributed to either $\omega_{1,h}$ or $\omega_{2,h}$ defined in (2.18) and (2.20), respectively.

Example 1. As our first example, we consider the eigenvalue problem (2.2) with $\Omega = (0,1) \times (0,1)$. In this case, $\lambda = 2\pi^2$, and its corresponding eigenfunction is $u = 2\sin(\pi x)\sin(\pi y)$. We consider both structured and unstructured meshes.

In order to generate structured meshes, we divide Ω into $m \times m$ subsquares and triangulate each subsquare to one of the patterns shown in Figure 3.1. In consecutive iterations, $m = 16, 32, 64, 128$ for the criss cross pattern, while $m = 8, 16, 32, 64$ for the other three patterns. The numerical results for each of the four patterns are shown in Figures 3.2–3.5.

Let us have a closer look at Figure 3.2. First, the recovered gradient $\mathrm{G_h}\, u_h$ superconverges to ∇u. Accordingly, the convergence rate for $\omega_{1,h}$ is $O(h^3)$ if the Cauchy–Schwartz inequality is applied. However, this rate is $O(h^4)$ as depicted in Figure 3.2; i.e., $\omega_{1,h}$ is superconvergent. Consequently, all the terms in the identity for $\lambda_h^* - \lambda$ enjoy superconvergence. Hence, $\lambda_h^* - \lambda$ gets the ultraconvergence rate $O(h^4)$. Indeed, the same conclusion is true for the PPR in the other three cases.

As for the SPR, the situation is different. In the chevron pattern, the SPR-recovered gradient has no superconvergence [13]. Consequently, there is no superconvergence in $\lambda_h^* - \lambda$ although λ_h^* is more accurate than λ_h. In the Union Jack and the criss cross patterns, $\omega_{1,h}$ and consequently λ_h^*, do not gain from the superconvergence in the SPR-recovered gradient.

Next, we use the Delaunay triangulation (see Figure 3.6) to produce an unstructured initial mesh. In consecutive refinement, we construct a new mesh from the previous one by regular refinement, i.e., dividing each triangle into four congruent subtriangles by connecting its three edge centers. Figure 3.7 shows the convergence rates for various quantities of interest. Note that the recovered eigenvalue still has ultraconvergence. Surprisingly, the convergence rate is even better than the ones we have seen in the case of structured meshes, even though the recovered gradient does not have a full order recovery.

Example 2. So far, we have seen that $\omega_{1,h}$ and $\omega_{2,h}$ are almost the same. There are situations where the cancellations in $\omega_{2,h}$ are better, as we can see from the following example:

$$\begin{cases} -\triangle u = \lambda u \qquad \text{in } \Omega = (0,1)^2, \\ u|_{x=0} = u|_{y=0} = u|_{y=1} = \partial_x u|_{x=1} = 0, \\ \|u\|_{L_2(\Omega)} = 1. \end{cases}$$

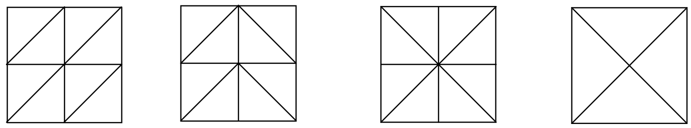

(a) The Regular pattern (b) The Chevron pattern (c) The Union Jack pattern (d) The Criss Cross pattern

FIG. 3.1. *The patterns used in constructing uniform meshes in* $\Omega = (0,1)^2$.

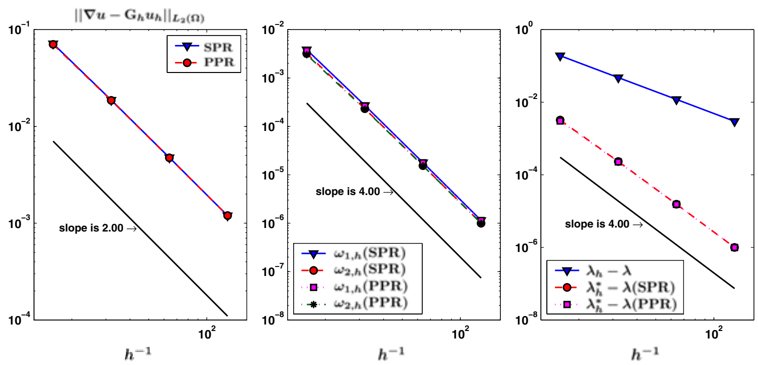

FIG. 3.2. *Example* 1 *results—the regular pattern case.*

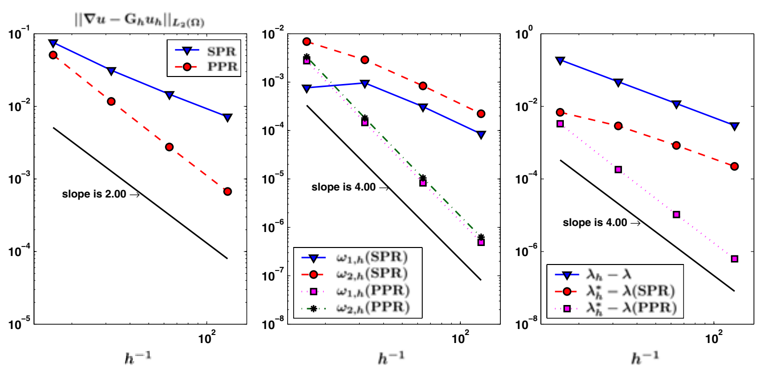

FIG. 3.3. *Example* 1 *results—the chevron pattern case.*

In this case,

$$\lambda = \frac{5\pi^2}{4}, \qquad u = 2\cos(\pi(x-1)/2)\sin \pi y.$$

Let us solve this problem using the sequence of meshes with an unstructured initial mesh employed in Example 1; see Figure 3.8 for the numerical results. As for the PPR, contrary to the SPR, the convergence rate of $\omega_{1,h}$ is less than the convergence rate of $\omega_{2,h}$ by at least 1. This means that η_h cancels not only the leading term in $\|\nabla e_h\|_{0,\Omega}$, but also the major part of $\frac{\lambda\|e_h\|_{0,\Omega}^2}{2\eta_h}$. This leads to a higher convergence rate in the recovered eigenvalue. Likewise, the dot product term in (2.19) cancels the first term in a favorable way since both terms are not as good as $O(h^4)$ and the enhanced eigenvalue converges at a rate $O(h^5)$!

Example 3. In our previous two examples, the domain was a unit square. Let us

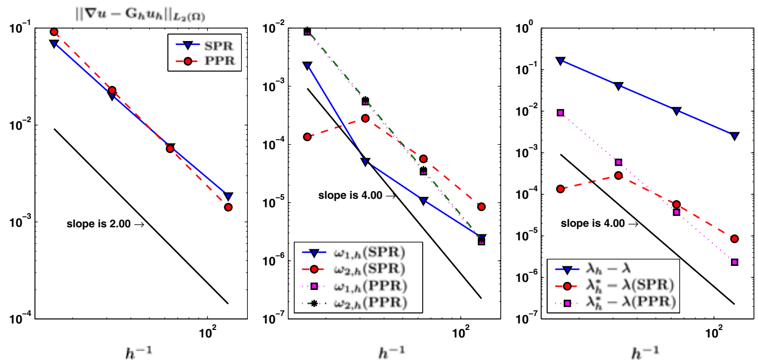

FIG. 3.4. *Example* 1 *results—the Union Jack pattern case.*

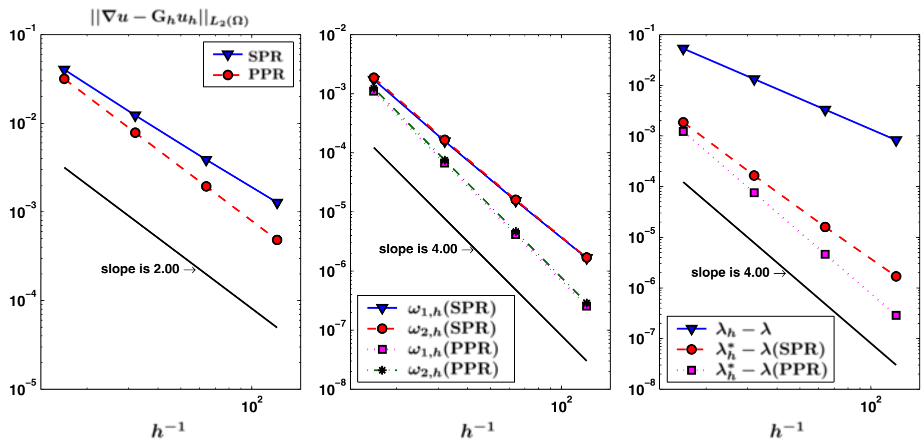

FIG. 3.5. *Example* 1 *results—the criss cross pattern case.*

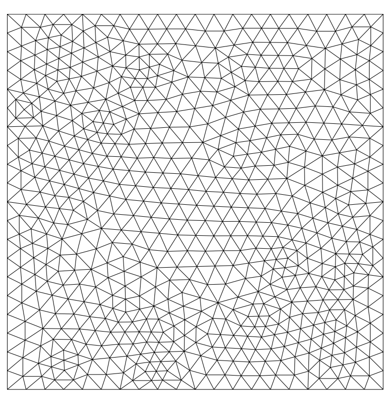

FIG. 3.6. *Example* 1*—the initial unstructured mesh case.*

change the domain to an equilateral triangle:

$$\Omega = (x, y) \in \mathbb{R}^2 : 0 < y < \sqrt{3}x, y > \sqrt{3}(1 - x).$$

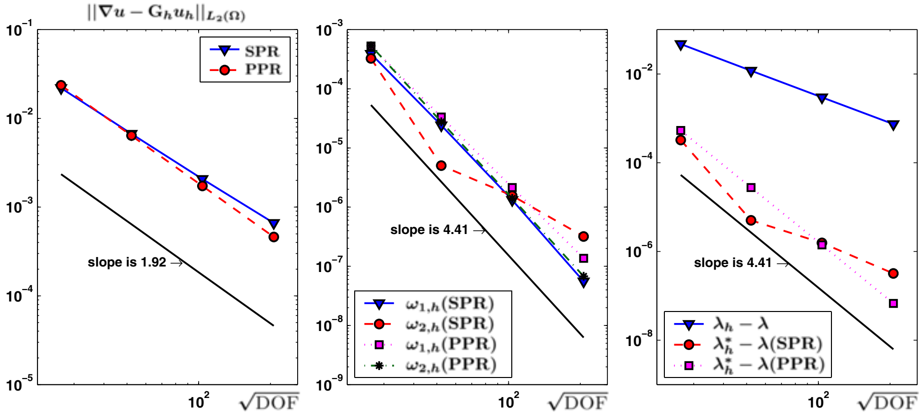

FIG. 3.7. *Example* 1 *results—the unstructured mesh case.*

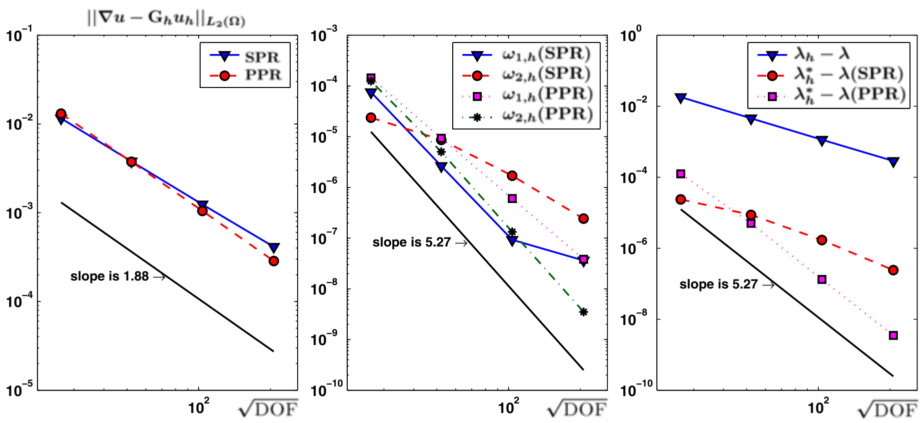

FIG. 3.8. *Example* 2 *results.*

With the zero boundary condition, $\lambda = 16\pi^2/3$ and

$$u = \frac{2\sqrt[4]{12}}{3}\left\{\sin\left(\frac{4\pi y}{\sqrt{3}}\right) + \sin\left(2\pi\left(x - \frac{y}{\sqrt{3}}\right)\right) + \sin\left(2\pi\left(1 - x - \frac{y}{\sqrt{3}}\right)\right)\right\}.$$

The structured meshes are generated by dividing Ω into $m(m+1)/2$ equilateral triangles with $m = 2^k$ for $k = 4, 5, 6, 7$. The initial mesh is shown in Figure 3.9. For unstructured initial mesh, we do as in Example 1 (see Figure 3.10.) The numerical results for both types of meshes are shown in Figures 3.11 and 3.12, respectively. Obviously, the results are similar to the ones in Example 1. Due to the high quality of the initially unstructured triangulation, there is not much difference between the convergence rates for uniform and unstructured meshes in this case.

Example 4. In all previous examples, the eigenfunction u was analytic. Let us now consider the model problem (2.1) with

$$\Omega = \{(r, \theta) \in \mathbb{R}^2 : \ 0 < r < 1, \ \ 0 < \theta < 3\pi/2\},$$

in which case u has a corner singularity at $(0, 0)$. The smallest eigenvalue and its

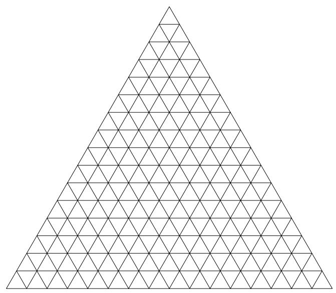

FIG. 3.9. *Example 3—the initial structured mesh.*

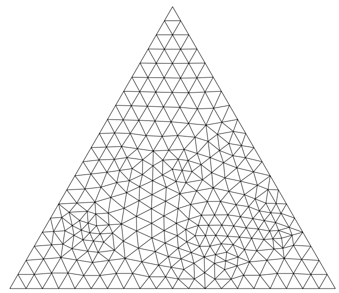

FIG. 3.10. *Example 3—the initial unstructured mesh.*

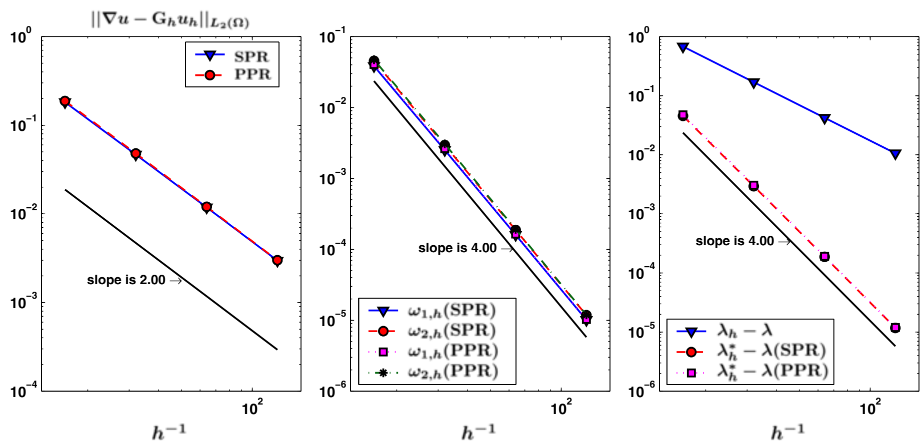

FIG. 3.11. *Example 3 results—the structured mesh case.*

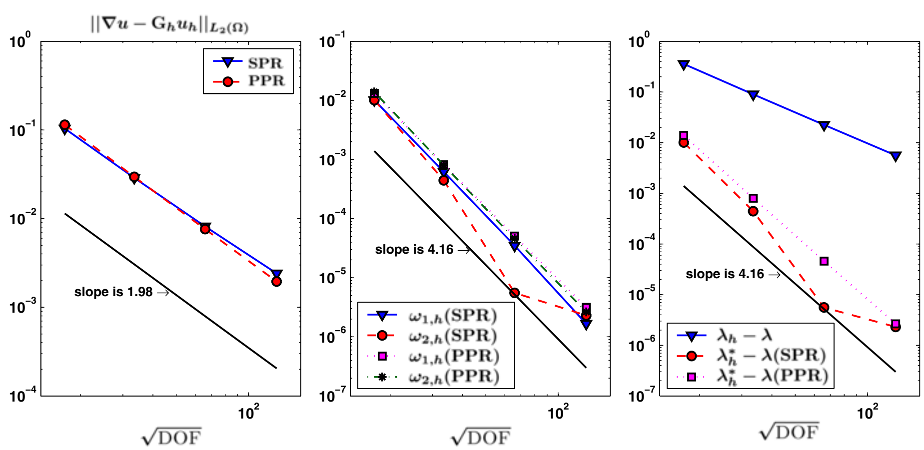

FIG. 3.12. *Example 3 results—the unstructured mesh case.*

eigenfunction for this problem are

$$u(r,\theta) = \frac{4J_{2/3}(\alpha r)}{\sqrt{6\pi}J_{5/3}(\alpha)}\sin(2\theta/3), \qquad \lambda_{\min} = \alpha^2, \qquad \alpha = \min\{x > 0 : J_{2/3}(x) = 0\},$$

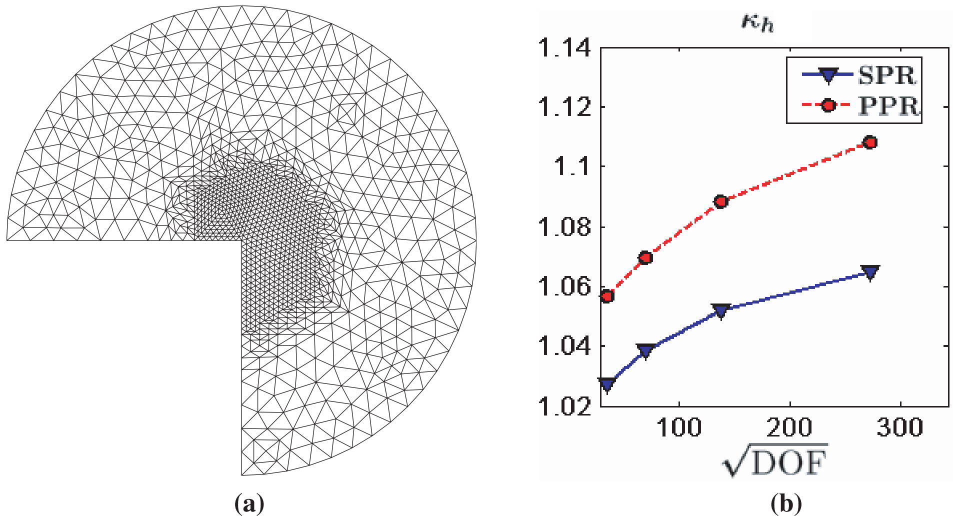

FIG. 3.13. *Example* 4*—the initial mesh* (a) *and the effectivity index* (b).

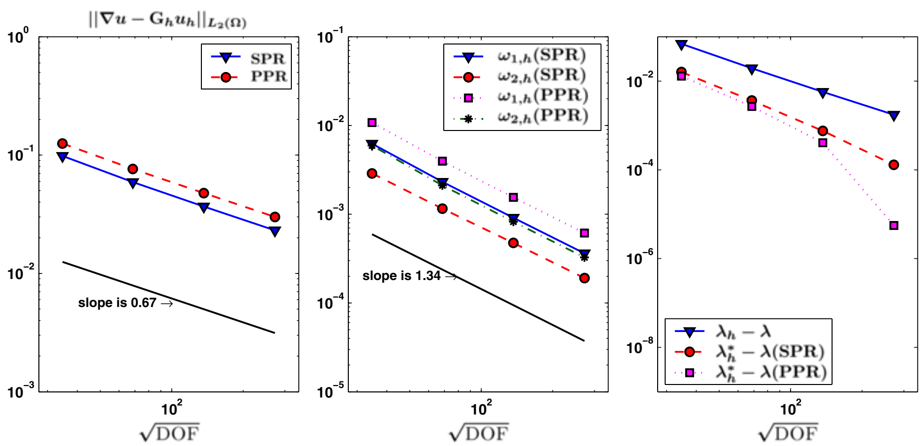

FIG. 3.14. *Example* 4 *results.*

where $J_{2/3}$ is the Bessel function of the first kind of order $2/3$. We start from an initial mesh shown in Figure 3.13(a). Note that this mesh is refined near $(0,0)$ to avoid the pollution effect of the corner singularity. A sequence of meshes is produced by the regular refinement; i.e., by linking the three edge centers, each triangle is divided into four congruent subtriangles. From the numerical results in Figure 3.14, $\mathrm{G_h}\, u_h$ does not have superconvergence in both the PPR and the SPR. Nevertheless, η_h is still close to $\|\nabla e_h\|_{0,\Omega}$ (see the effectivity index $\kappa_h := \eta_h/\|\nabla e_h\|_{0,\Omega}$ in Figure 3.13(b)). From (2.10), the leading term in $\lambda_h^* - \lambda$ is $|\|\nabla e_h\|_{0,\Omega}^2 - \eta_h^2| = \|\nabla e_h\|_{0,\Omega}^2 |1 - \kappa_h^2|$. Since κ_h is very close to 1, the error in $\lambda_h^* - \lambda$ is a small fraction of the exact error $\lambda_h - \lambda$, which means that λ_h^* is more accurate than λ_h. This is true for both the PPR and the SPR.

4. Conclusion. We have shown that the PPR-recovered gradient $\mathrm{G_h}\, u_h$ can enhance the accuracy of λ_h if $\mathrm{G_h}\, u_h$ superconverges to ∇u (as we have seen in Examples 1, 2, and 3) or if the effectivity index of η_h is close to 1 (as we have seen in Example 4). Although the numerical results in this work are solely for the two-dimensional Poisson equation and the linear finite element method, the idea is nevertheless applicable to more general eigenvalue problems in the form

$$a(u, v) = \lambda b(u, v). \tag{4.1}$$

Here $a(\cdot,\cdot)$ and $b(\cdot,\cdot)$ are symmetric bilinear forms on some Hilbert space H and satisfy certain strong ellipticity and positivity conditions such that the following basic identity is valid (see [3, Lemma 9.1]):

$$\tilde{\lambda} - \lambda = \|u - w\|_a^2 - \lambda \|u - w\|_b^2,$$

where (u, λ) is an eigenpair of (4.1) with $\|u\|_b = 1$, $w \in H$ with $\|w\|_b = 1$, and $\tilde{\lambda} = a(w, w)$. In this setting, let $(\tilde{\lambda}, w) = (\lambda_h, u_h)$ be the finite element approximation of (u, λ). If we are able to improve the quantity involving u in the $\|\cdot\|_a$-norm via a recovery procedure, then $\|u - u_h\|_a^2$ may be substituted by a computable value to enhance the eigenvalue approximation. Further investigation along this line for the linear and the nonlinear problems is under way.

REFERENCES

[1] M. Ainsworth and J. T. Oden, *A Posteriori Error Estimation in Finite Element Analysis*, Wiley Interscience, New York, 2000.

[2] I. Babuška and T. Strouboulis, *The Finite Element Method and Its Reliability*, The Clarendon Press, Oxford University Press, New York, 2001.

[3] I. Babuška and J. E. Osborn, *Eigenvalue problems*, in Handbook of Numerical Analysis, Vol. II, Finite Element Methods (Part I), Handb. Numer. Anal. II, P. G. Ciarlet and J. L. Lions, eds., North–Holland, Amsterdam, 1991, pp. 641–787.

[4] F. Chatelin, *Spectral Approximations of Linear Operators*, Academic Press, New York, 1983.

[5] W. Dörfler and R. H. Nochetto, *Small data oscillation implies the saturation assumption*, Numer. Math., 91 (2002), pp. 1–12.

[6] A. Naga and Z. Zhang, *A posteriori error estimates based on the polynomial preserving recovery*, SIAM J. Numer. Anal., 42 (2004), pp. 1780–1800.

[7] A. Naga and Z. Zhang, *The polynomial-preserving recovery for higher order finite element methods in 2D and 3D*, Discrete Contin. Dyn. Syst. Ser. B, 5 (2005), pp. 769–798.

[8] L. Shen and A. Zhou, *A defect correction scheme for finite element eigenvalues with applications to quantum chemistry*, SIAM J. Sci. Comput., 28 (2006), pp. 321–338.

[9] J. Xu and Z. Zhang, *Analysis of recovery type a posteriori error estimators for mildly structured grids*, Math. Comp., 73 (2004), pp. 1139–1152.

[10] J. Xu and A. Zhou, *A two-grid discretization scheme for eigenvalue problems*, Math. Comp., 70 (2001), pp. 17–25.

[11] Y. Yang, *An Analysis of the Finite Element Method for Eigenvalue Problems*, Guizhou Press, Guiyang, China, 2004 (in Chinese).

[12] Z. Zhang, *Polynomial preserving gradient recovery and a posteriori estimate for bilinear element on irregular quadrilaterals*, Int. J. Numer. Anal. Model., 1 (2004), pp. 1–24.

[13] Z. Zhang and A. Naga, *A new finite element gradient recovery method: Superconvergence property*, SIAM J. Sci. Comput., 26 (2005), pp. 1192–1213.

[14] O. C. Zienkiewicz and J. Z. Zhu, *The superconvergent patch recovery and a posteriori error estimates.* I. *The recovery technique*, Internat. J. Numer. Methods Engrg., 33 (1992), pp. 1331–1364.

[15] O. C. Zienkiewicz and J. Z. Zhu, *The superconvergent patch recovery and a posteriori error estimates.* II. *Error estimates and adaptivity*, Internat. J. Numer. Methods Engrg., 33 (1992), pp. 1365–1382.